Supplementary Information (SI) for Analytical Methods.
This journal is © The Royal Society of Chemistry 2026

Supporting Information for

An Al^{3+} Ions-Responsive Blue Emitting Ionic Liquid-Based Nano-Optode and Its Implications for the Detection of 2, 4, 6-Trinitrophenol

Shubham Lama and Sudhir Kumar Das*

Department of Chemistry, University of North Bengal, Raja Rammohunpur, Darjeeling,

West Bengal-734013, India

*Corresponding author (Dr. S. K. Das, E-mail: sudhirkumardas@nbu.ac.in)

Table of Contents

Experimental section

General methods and instrumentation

Chemical reagents were procured from Sigma-Aldrich, India, and applied without any further purification. Anhydrous solvents and HPLC-grade solvents for spectroscopy were obtained from Merck, India. We have purchased all of the cationic and anionic salts from Sigma-Aldrich in India, including trihexyltetradecylphosphonium chloride [TTP][Cl] and Nicotinic hydrazide. Also, Deuterated chloroform (DMSO-d_6) was purchased from Sigma-Aldrich, India, and used for NMR spectroscopic analysis. Fourier transform infrared (FT-IR) spectra were recorded using a Bruker Optik GMBH (Germany) FT-IR spectrometer under ambient conditions. Mass spectrometric analysis was performed on a Quattro Micro API (MICROMASS, UK) coupled with an LC-WATERS 2695 system equipped with a PDA2998 detector, ESI_Negative with capillary voltage 3 kV, Cone -30 V and extractor-3 V employing source and dissolving temperature -90℃ and -250℃ respectively using dissolving gas-450 Litre/hour with flow rate-10 μL/min. We used a HITACHI U-2910 spectrophotometer for monitoring UV-visible absorption spectra, while fluorescence measurements were performed on a HITACHI F-7100 fluorimeter, employing a 5 nm slit width for both excitation and emission. During steady-state emission studies, the excitation wavelength was set to 330 nm, and emission was monitored over 330–640 nm. The size and shape of the **nHNMIL** are estimated by field emission scanning electron microscopy (SEM) (ZEISS) employing an operating voltage of 50 kV by drop casting the required amounts of **nHNMIL** (20 μg/mL) on the carbon-coated copper grids. The average particle size is determined by considering the size of more than 100 particles. The hydrodynamic radius of **nHNMIL** is measured employing the High-resolution Photon Correlation Spectroscopy (PCS) technique (Anton Paar Litesizer 500). The zeta potential (ζ) of nanoparticles is also obtained by this instrument using a capillary ζ-cell.

Before the analysis, the HNMIL stock solution was prepared immediately (1×10^{-3} M in DMSO). The solution of numerous inorganic metal salts like $AlCl_3$, $BaCl_2$, $CaCl_2$, $CdCl_2$, $CoCl_2$, $CuCl_2$, $ZnCl_2$, $FeCl_3$, $HgCl_2$, $MgCl_2$, $MnCl_2$, $NiCl_2$, $PbCl_2$, and $FeCl_2$ including all the inorganic and organic anion salt like $AlPO_4$, K_2CO_3, KBr, KCl, NaF, $NaBPh_4$, Na_2HPO4, NaH_2PO_4, Na_3PO_4, KPF_6, S^{2-} and Na_2SO_4 were prepared instantly in (1×10^{-4} M) concentration in water.

For the fabrication of paper-based test kit, Whatman-41 filter paper is cut into strips, which are fully immersed in **nHNMIL** aqueous solution (85 μM) for a while. Finally, the test strips are removed and dried in a hot air oven at 60 °C. Some drops of each metal ion solution (10^{-3} M) are added to these filter papers.

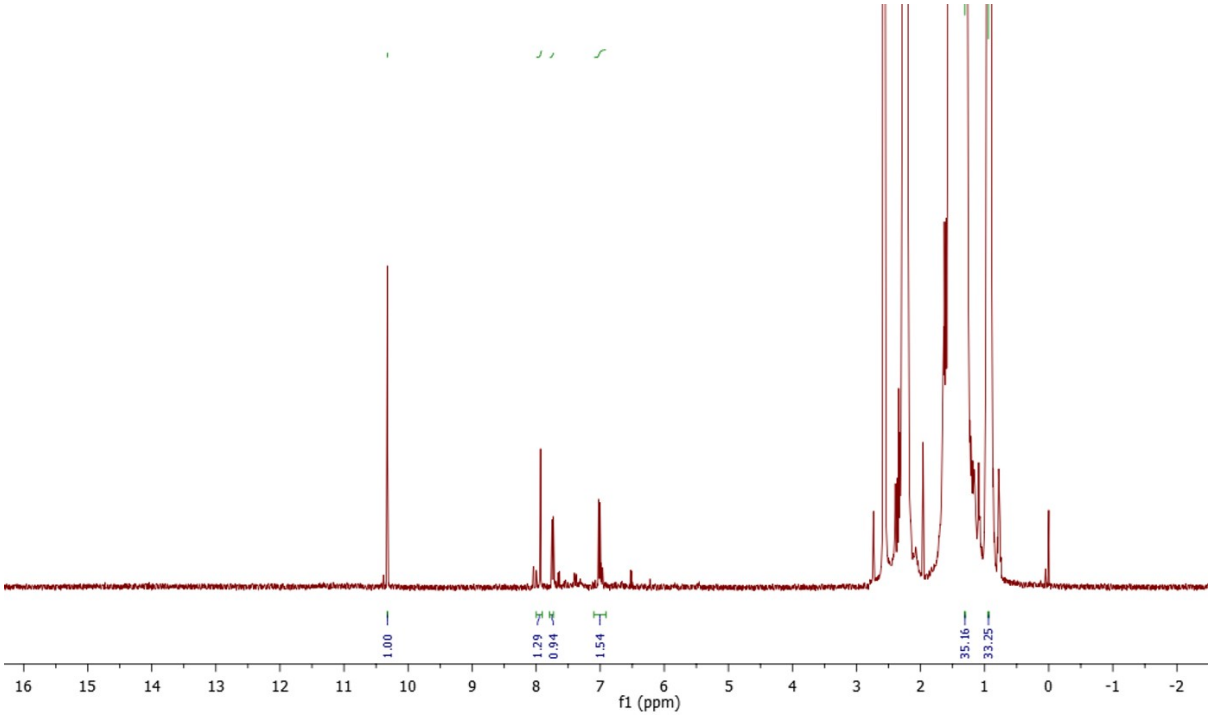

Fig. S1: ^{1}H NMR spectrum (DMSO-d_6, 400 MHz) of **[TTP][FHS]**.

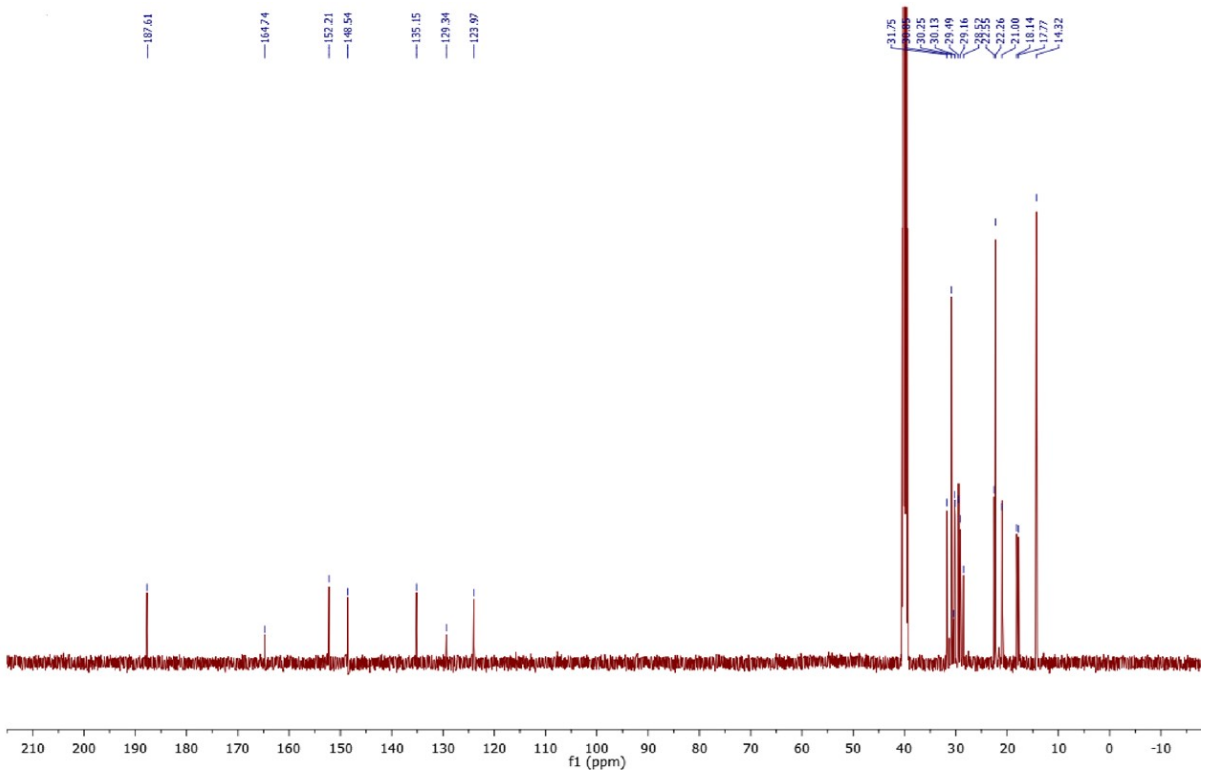

Fig. S2: ^{13}C NMR spectrum (DMSO-d_6, 100 MHz) of **[TTP][FHS]**.

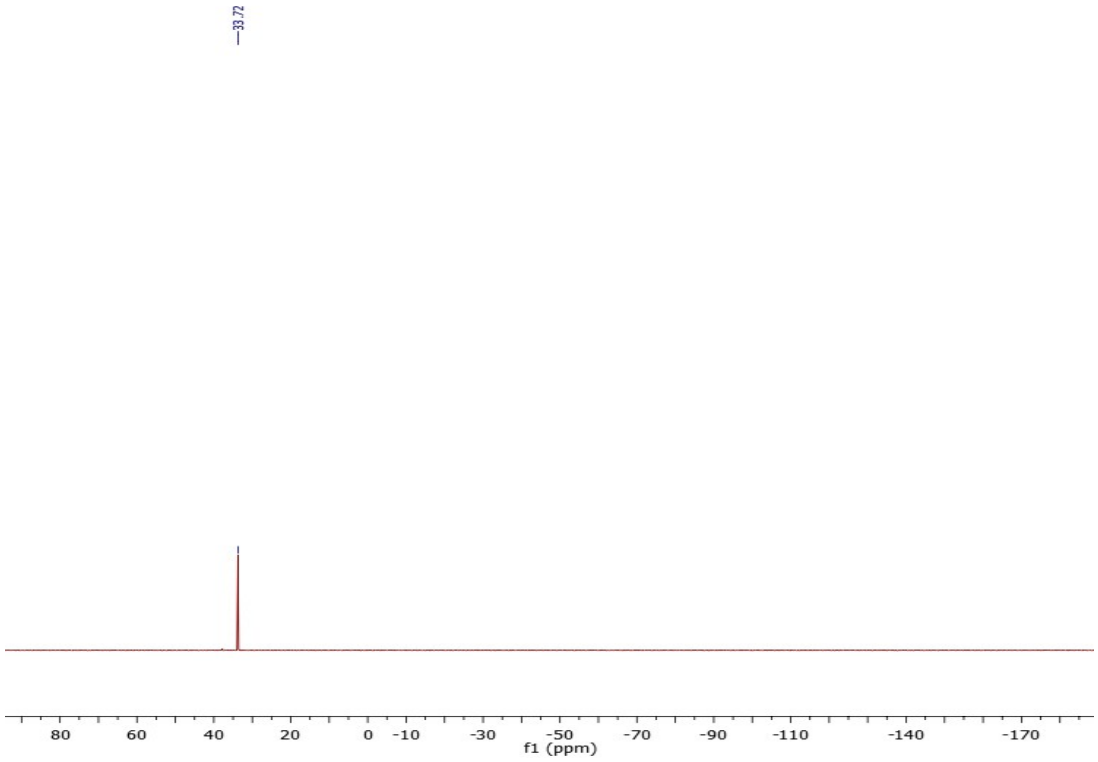

Fig. S3: ^{31}P NMR spectrum (DMSO-d_6, 400 MHz) of **[TTP][FHS]**.

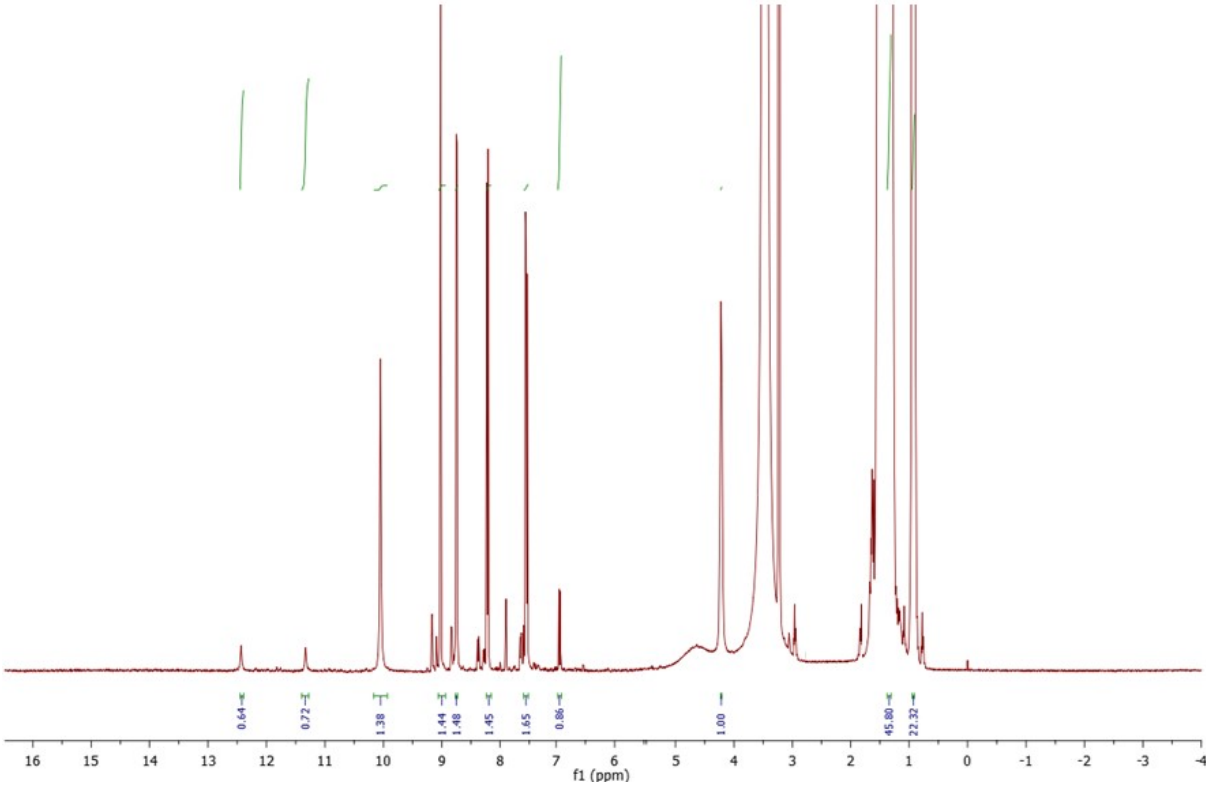

Fig. S4: ^{1}H NMR spectrum (DMSO-d_6, 400 MHz) of **HNMIL**.

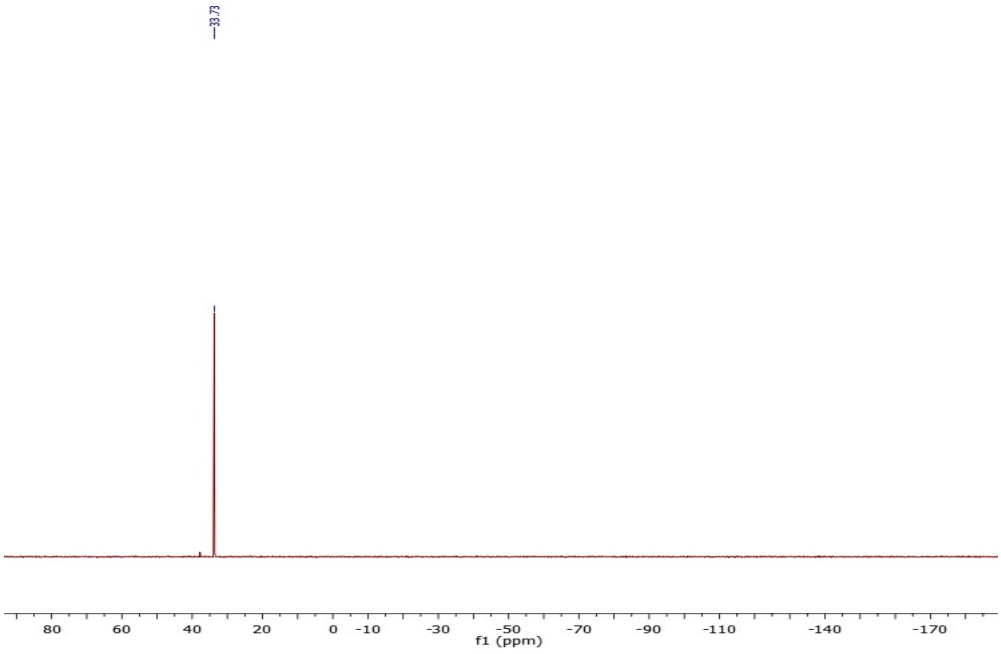

Fig. S5. ^{31}P NMR spectrum (DMSO-d_6, 400 MHz) of **[TTP][FHS]**.

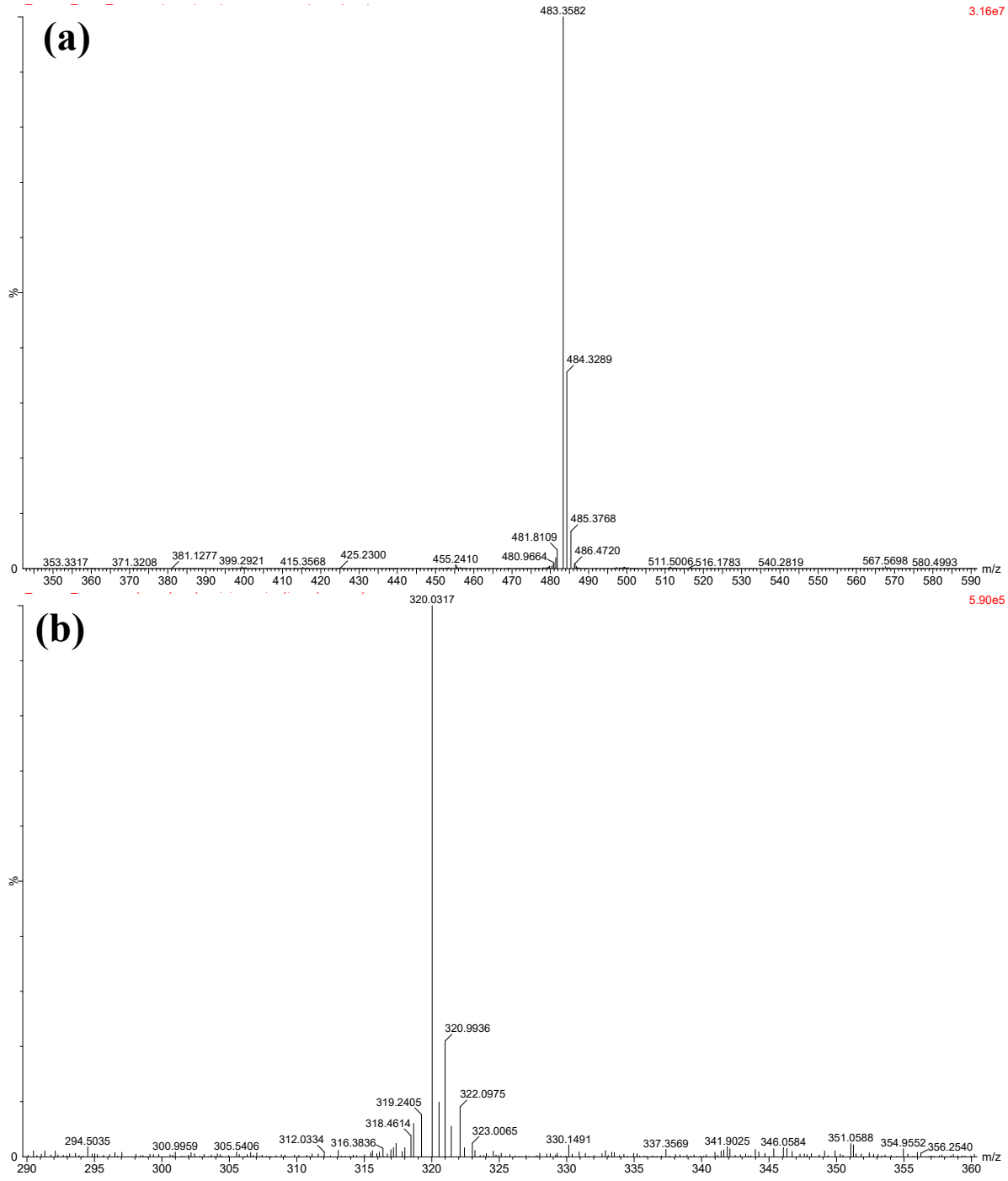

Fig. S6: LC-MS spectra of **HDIL (a)** positive ion mode and **(b)** negative ion mode.

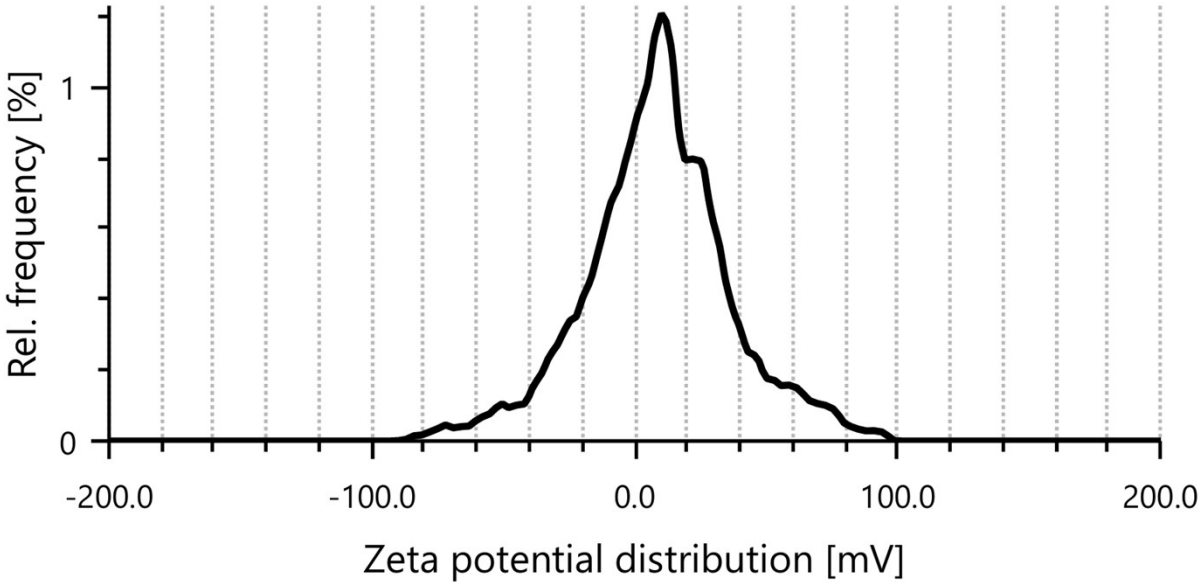

Fig. S7: The relative frequency vs. zeta potential distribution curve for the determination of the zeta potential of **nHNMIL**.

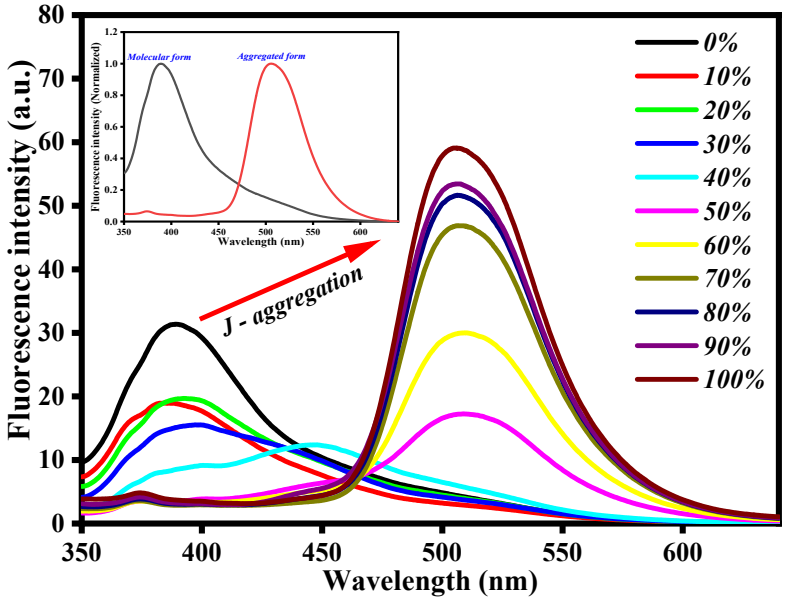

Fig. S8: Fluorescence spectra of **HNMIL** in water-DMSO mixed solvents demonstrating red shift.

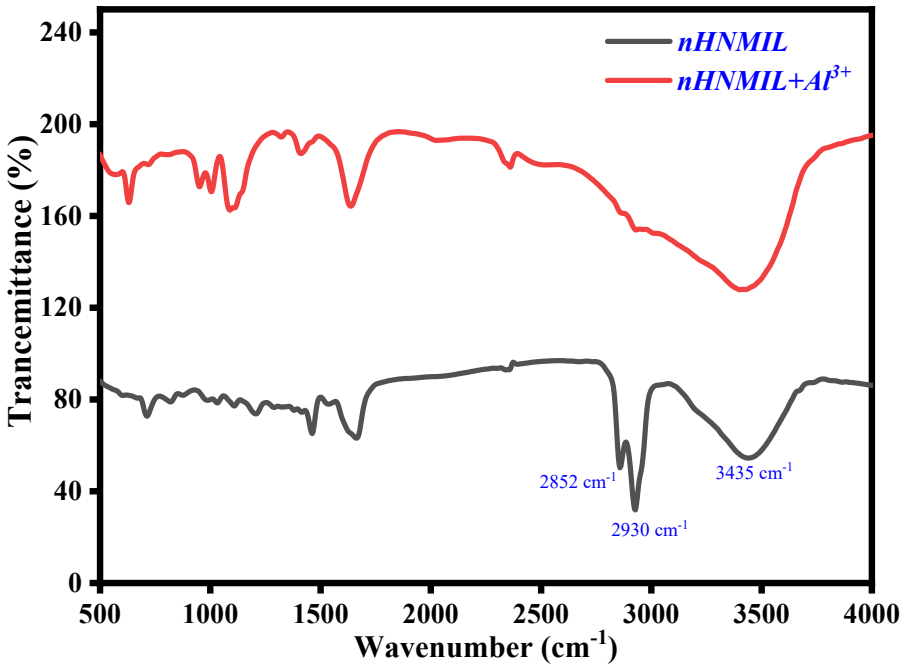

Fig. S9: FT-IR spectra of **nHNMIL** before and after the interaction with Al^{3+} ions.

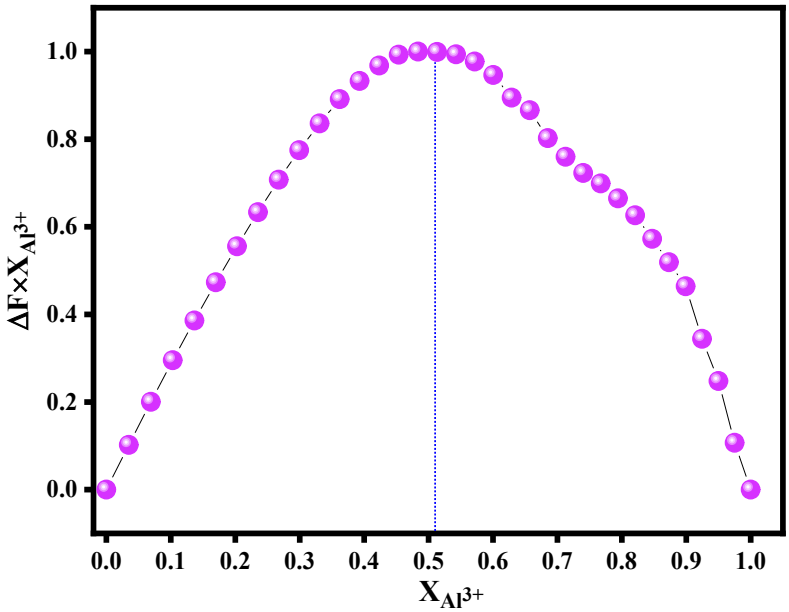

Fig. S10: Job's plot demonstrating the 1:1 stochiometric ratio, interaction of Al^{3+} ion with **nHNMIL**.

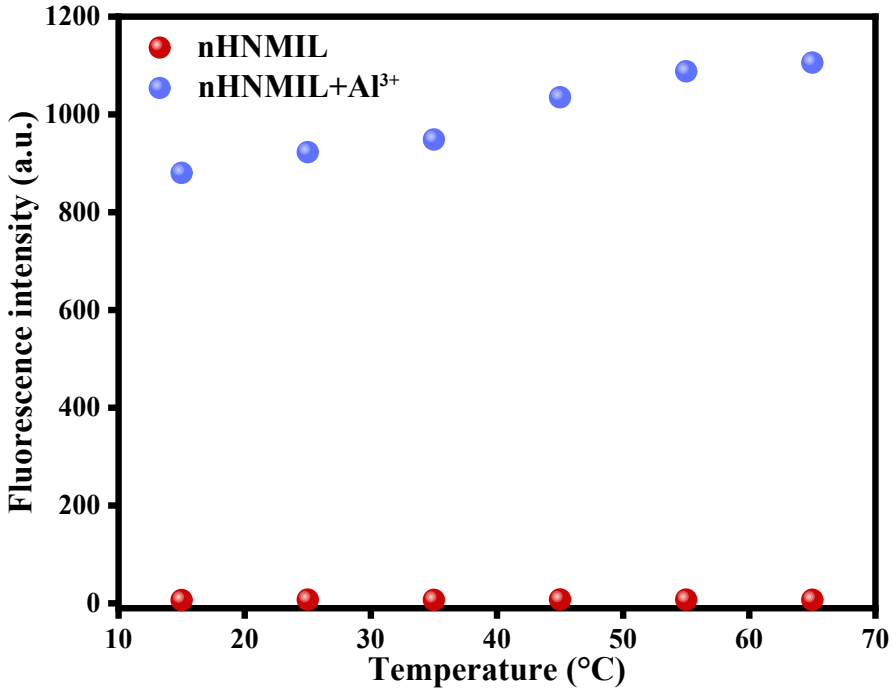

Fig. S11: Temperature-dependent fluorescence study of **nHNMIL** and **nHNMIL-**Al^{3+} complex.

Table S1. Calculated ΔG values at various temperatures.

Temperature(℃)	**ΔG** (J mol^{-1})	**ΔH** (J mol^{-1})	**ΔS** (J mol^{-1} K^{-1})
15	-23497.62858	-22273	81.59
25	-24313.51846		
35	-25129.40835		
45	-25945.29823		
55	-26761.18811		
65	-27577.07799		

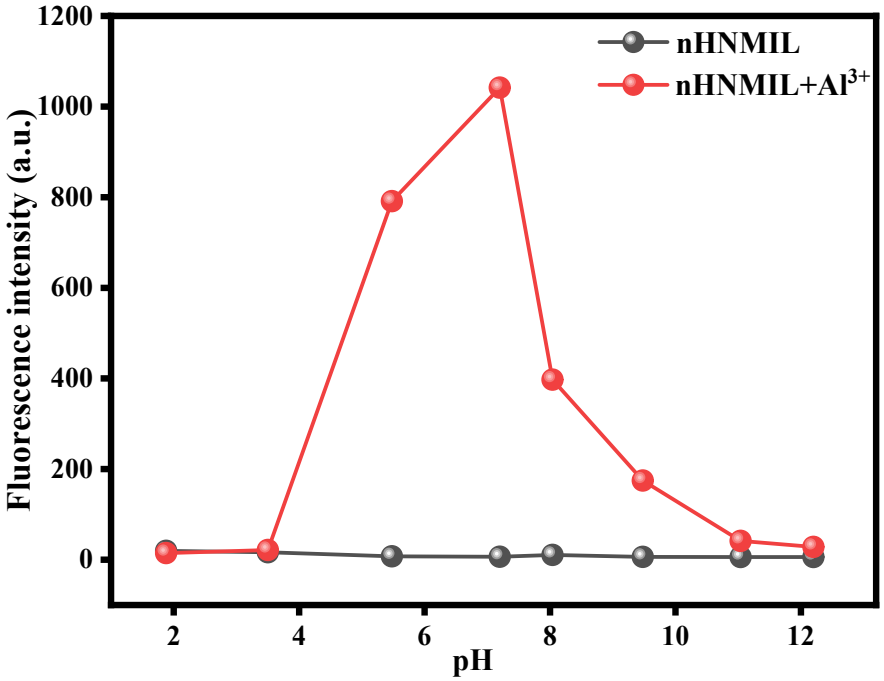

Fig. S12: pH study of **nHNMIL** and **nHNMIL**-Al^{3+} complex.

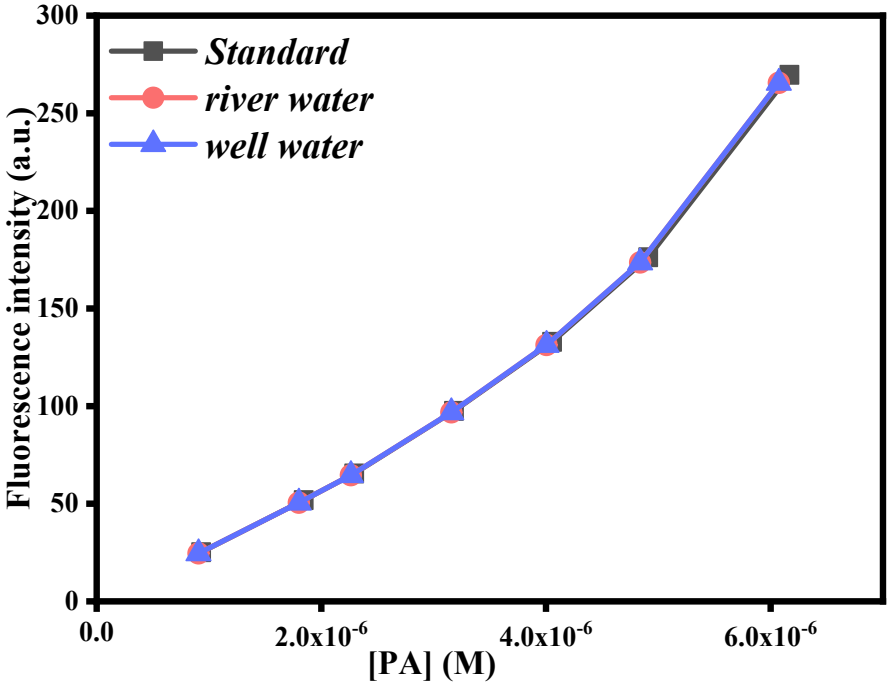

Fig. S13: Calibration curve for determining Al^{3+} contamination in different water samples.

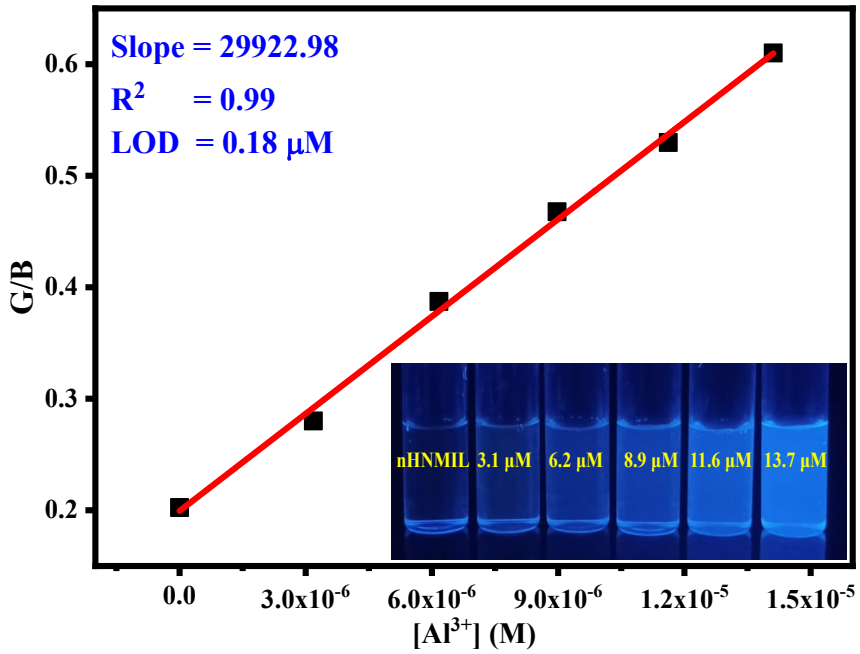

Fig. S14: The calibration curve of G/B vs. [Al^{3+}] using a smartphone-based method under 365-nm UV irradiation, shot by Vivo Y31-S smartphone.

Table S2: Quantitative comparison between smartphone-based measurements and laboratory fluorimeter data.

Sl. no	[Al]	G/B		Laboratory fluorimeter data (a.u.)
		Realme 6	Vivo Y31-S	
1.	0	0.22368	0.20237	4.718
2.	3.1	0.34	0.28	211
3.	6.2	0.41727	0.38727	443
4.	8.9	0.48765	0.46765	669
5.	11.6	0.58974	0.52974	861
6.	13.7	0.65	0.61	1017
LOD		**0.1 µM**	**0.18 µM**	**48 pM**

Table S3: Determination of Al^{3+} in water samples.

Sample	Added (µM)	Found (µM)	Recovery (%)
River water	0.93	0.92	99.007

	1.84	1.78	97.02
	2.3	2.27	98.99
	3.2	3.11	98.00
	4.05	4.01	99.09
	4.9	4.86	99.09
	6.2	6.09	98.85
Well water	0.93	0.90	97.53
	1.84	1.79	97.62
	2.3	2.26	98.70
	3.2	3.15	99.25
	4.05	4	98.79
	4.9	4.8	98.52
	6.2	6.07	98.47

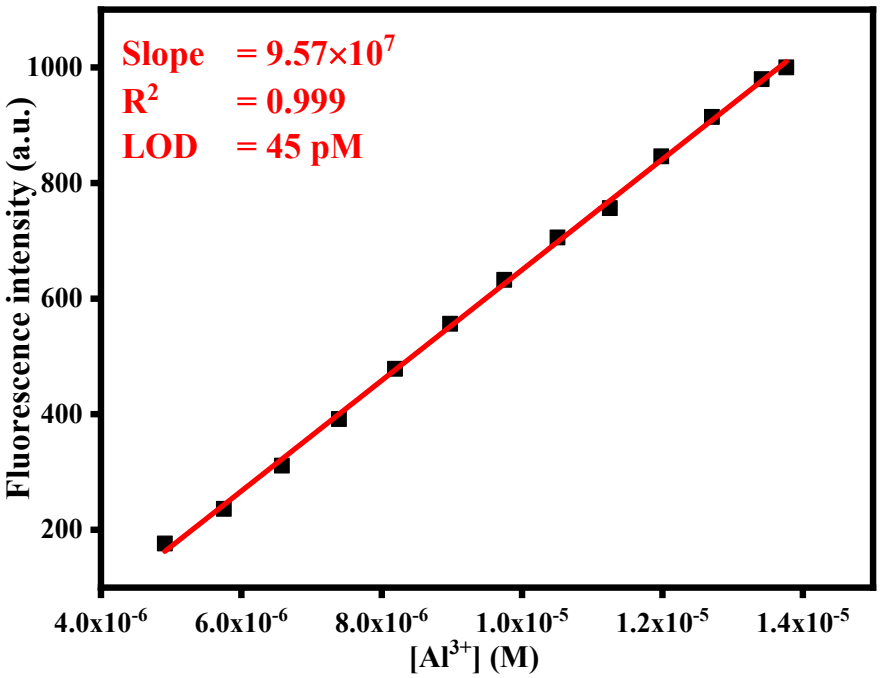

Fig. S15: Estimation of LOD in real matrix (River water).

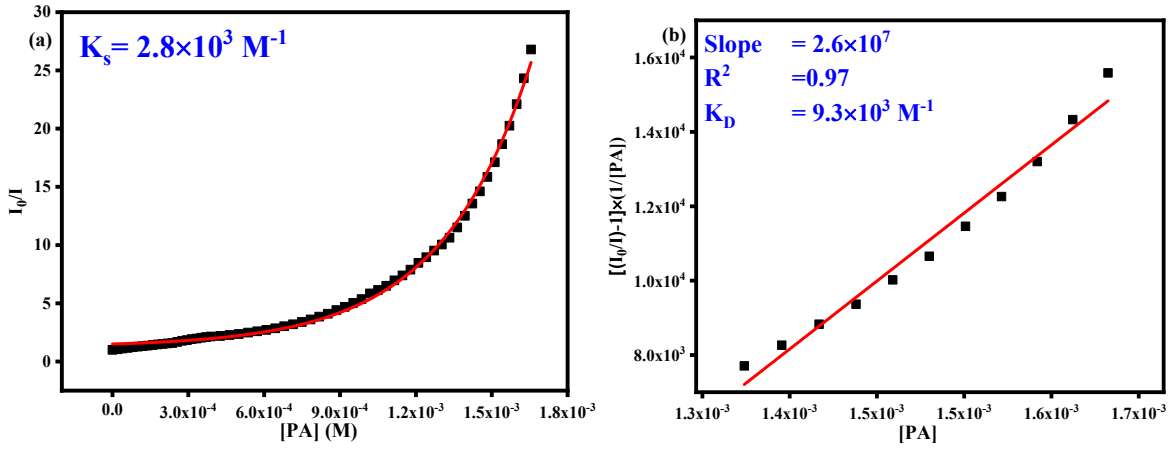

Fig. S16: Plot demonstrating the interaction of PA with our formulated **nHNMIL**-Al^{3+} complex (**a**) statically and (**b**) dynamically.

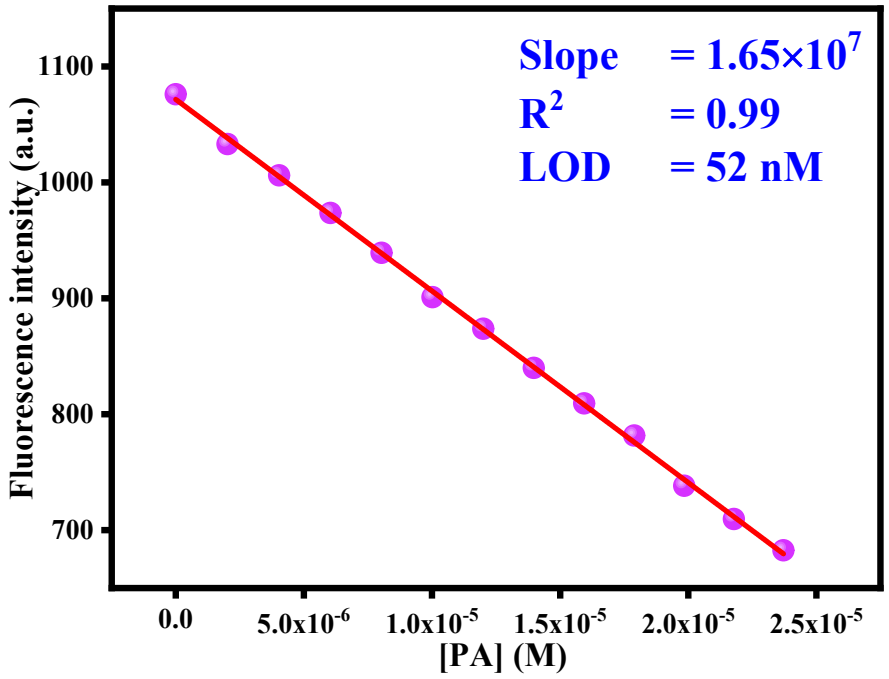

Fig. S17. Detection limit of PA with our formulated **nHNMIL**-Al^{3+} complex.

Table S4: Comparison table of different chemosensors that have been introduced for detecting Al^{3+} ions in the last few decades, with our prepared **nHNMIL**.

Structure	solvent	LOD	Sensory type	Response time	Ref
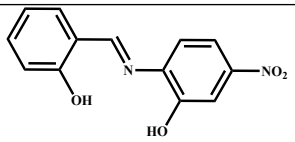	DMF	9.45 nM	Ratiometric	within a few seconds	1

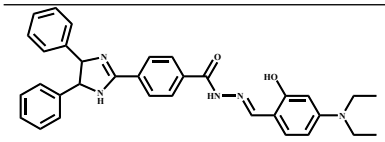	EtOH/H_2O (1:1)	74.75 nM	Turn-on	~10 min	2
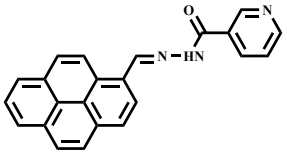	DMSO H2O,	0.17 μM	Turn-on	-	3
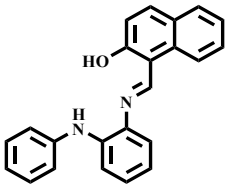	THF/H2O, 1:1 (v/v), HEPES =50 mM, pH =7.4	0.02 μM	Turn-on	<10 s	4
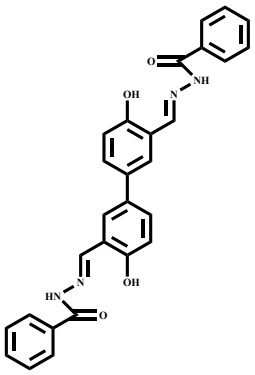	Methanol–water medium	3.50 nM	Turn-on	Rapid response	5
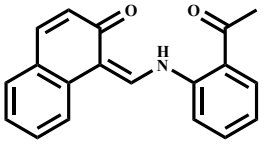	EtOH	0.013 ppm	Turn-off	rapid response	6
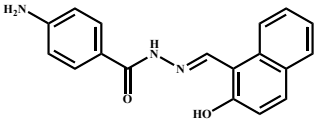	Aqueous/environmental samples	6.7 nM	Turn-on	≤3 min	7
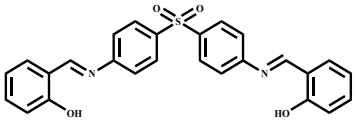	20 % (v/v) water-DMSO medium	15 nM	Turn-on	rapid response	8
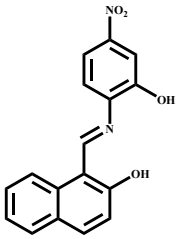	DMF	8.6 nM	Turn-on	rapid response	9
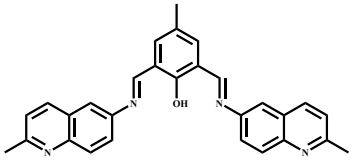	DMSO/H_2O (7:3)	1.11 μM	Turn-on	Fast response	10

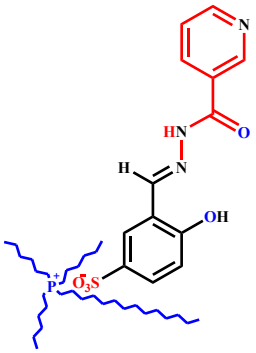	**Water dispersion**	**37 pM**	**Turn-on**	**Within few sec**	**This work**

Table S5: Comparison with the detection limits of sensing PA by various sensors.

System	LOD	References
HL-Al3^{+} complex	0.623 µM	[11]
ZnSe quantum dots	12.4 µM	[12]
ZnO nanoparticles	7.8 µM	[13]
Dabsyl derivative	7.2 µM	[14]
bluish-green fluorescent histidine	2.72 µM	[15]
Dy(III)-based MOFs	7.1 µM	[16]
Phenanthroimidazole derivatives	2.3-4.6 µM	[17]
carbon dots	0.63 µM	[18]
FRET-based rhodamine derivative	0.82 µM	[19]
anthracene-bridged poly (N-vinyl pyrrolidone)	6 µM	[20]
Ionic liquid-based nano-optode	52 nM	**This work**

References

1 M. Rajbanshi, M. Mahato, J. Chourasia, S. Ghanta, and S. K. Das, *J. Mol. Struct.*, 2023, **1284**, 135357.

2 J. Wang, L. Ren, Y. Liu, P. Wang, Y. Chen and D. Zhang, *J. Fluoresc. 2025 3512*, 2025, **35**, 13267–13278.

3 Heena, A. Silswal, D. Sharma, A. L. Koner, H. Om, and R. Rana, *Spectrochim. Acta Part A Mol. Biomol. Spectrosc.*, 2024, **320**, 124575.

4 T. J. Dathees, S. P. Makarios Paul, A. Sanmugam, A. Abiram, S. Murugan, R. S. Kumar, A. I. Almansour, N. Arumugam, R. Nandhakumar, and D. Vikraman, *Spectrochim. Acta Part A Mol. Biomol. Spectrosc.*, 2024, **308**, 123732.

5 G. Kumar, I. Singh, R. Goel, K. Paul, and V. Luxami, *Spectrochim. Acta Part A Mol. Biomol. Spectrosc.*, 2024, **322**, 124784.

6 N. Apiratikul, P. Bunrit, S. Jommaroeng, P. Boonsri, and K. Songsrirote, *Sensors Int.*, 2025, **6**, 100313.

7 M. Liu, H. Zhu, Y. Fang, C. Liu, X. Li, X. Zhang, L. Ma, K. Wang, M. Yu, W. Sheng, and B. Zhu, *Spectrochim. Acta Part A Mol. Biomol. Spectrosc.*, 2024, **307**, 123578.

8 S. Ahamed, A. R. Das, J. Chourasia, S. Ali, S. Lama, S. Rai, U. Darnal, S. Pradhan, and S. K. Das, *J. Mol. Struct.*, 2025, **1333**, 141753.

9 P. Sarkar, M. Mahato, S. Ahamed, N. Tohora, M. Rajbanshi, J. Chourasia, A. Maiti, S. Ghanta, and S. Kumar Das, *Inorganica Chim. Acta*, 2024, **572**, 122273.

10 R. Bhowmick, P. Mondal and P. Chattopadhyay, *RSC Adv.*, 2023, **13**, 3394–3401.

11 M. Mahato, S. Mardanya, Z. Rahman, N. Tohora, P. Pramanik, S. Ghanta, A. A. Chowdhury, T. K. Shaw, and S. K. Das, *J. Photochem. Photobiol. A Chem.*, 2022, **433**, 114168.

12 V. Sharma and M. S. Mehata, *Spectrochim. Acta Part A Mol. Biomol. Spectrosc.*, 2021, **260**, 119937.

13 A. A. Ibrahim, P. Tiwari, M. S. Al-Assiri, A. E. Al-Salami, A. Umar, R. Kumar, S. H. Kim, Z. A. Ansari, and S. Baskoutas, *Mater. (Basel, Switzerland)*, DOI:10.3390/MA10070795.

14 P. Kumar, D. Arya, D. Nain, A. Singh, A. Ghosh, and D. A. Jose, *Dye. Pigment*, 2019,

166, 443–450.

15 R. Patel, S. Bothra, R. Kumar and S. K. Sahoo, *Nano-Structures & Nano-Objects*, 2019, **19**, 100345.

16 R. Rajak, M. Saraf, S. K. Verma, R. Kumar, and S. M. Mobin, *Inorg. Chem.*, 2019, **58**, 16065–16074.

17 R. Ahmed, A. Ali, M. Ahmad, A. Alsalme, R. A. Khan, and F. Ali, *New J. Chem.*, 2020, **44**, 20092–20100.

18 A. Kathiravan, A. Gowri, V. Srinivasan, T. A. Smith, M. Ashokkumar and M. Asha Jhonsi, *Analyst*, 2020, **145**, 4532–4539.

19 A FRET-based fluorescent and colorimetric probe for the specific Detection of picric acid - RSC Advances (RSC Publishing) DOI:10.1039/C8RA05468A, https://pubs.rsc.org/en/content/articlehtml/2018/ra/c8ra05468a, (accessed 8 October 2025).

20 R. Singh, K. Mitra, S. Singh, S. Senapati, V. K. Patel, S. Vishwakarma, A. Kumari, J. Singh, S. K. Sen Gupta, N. Misra, P. Maiti and B. Ray, *Analyst*, 2019, **144**, 3620–3634.